

## **ACTIVE BRAKE TORQUE VARIATION COMPENSATION WITH SPEED SCHEDULING OF AN ELECTROMECHANICAL BRAKE**

<sup>1</sup>Lee, Chih Feng\* ; <sup>2</sup>Manzie, Chris

<sup>1</sup>Linköping University, Sweden; <sup>2</sup>The University of Melbourne, Australia

**KEYWORDS** – brake-by-wire, electromechanical brake, judder, brake torque variation, disc thickness variation

### **ABSTRACT**

An approach to attenuate the brake judder actively is proposed. The proposed judder compensation algorithm generates a clamp force command that attenuates the judder inducing brake torque variation. An electromechanical brake with high-bandwidth closed-loop clamp force tracking performance is utilised to follow the generated command, where the judder is compensated at its source. Experimental results are presented and the compensator is validated over fixed and varying wheel speeds with significant judder attenuation demonstrated.

### **INTRODUCTION**

One important design priorities in automotive brake development is to reduce the occurrence of judder, perceived by the driver as a vibration at the steering wheel, brake pedal or vehicle body during light braking in mid to high speeds (30 to 140 km/h). A large portion of brake development resources is typically allocated to address judder, where failure to achieve this goal may not only leads to major recalls and warranty claims, but also damages the company reputation.

Brake judder is a braking induced vibration due to brake torque variation (BTV) arises from irregularities in the brake disc [1]. It can be categorised into cold and hot (or thermal) judder. The majority of judder cases are cold judder caused by geometrical irregularities, including rotor runout, disc thickness variation and brake lining-rotor surface friction variation, and typically have one to two oscillations per wheel rotation [2]. One the other hand, hot judder is caused by thermal deformation or uneven thermal expansion of brake disc, and typically has higher vibration frequencies (6 to 20 oscillations for every wheel rotation) [2][3].

Current solutions for brake judder include replacing or resurfacing the brake disc, using softer brake pads [4], or redesigning the suspension and steering systems [5]. While the former two approaches are corrective measures (applied after the driver has experienced judder) and may lead to shorter component life, the latter approaches may affect vehicle handling and are only locally isolating the vibration, as the source of vibration is not eliminated.

To mitigate these shortfalls, an active solution for compensating the BTV directly at its source is desirable. In [6], an adaptive compensation algorithm is designed to generate a clamp force command that attenuates the BTV, and it is implemented on an electromechanical brake (EMB). The EMB offers several advantages, including high fidelity clamp force regulation, high-bandwidth closed-loop clamp force tracking and flexible software deployment platform [7][8]. However, one shortcomings of the adaptive compensation algorithm is the requirement of online wheel position measurements that are not available in production vehicles.

To alleviate the need of additional wheel position sensors, this paper proposes a speed-scheduled BTV compensator design based on the output regulation theory. Note that wheel speed measurements are readily available in most production-vehicles.

The paper is structured as follows. The next section describes a linearised closed-loop EMB model, followed by a brake corner model that describes the brake torque generation. These models serve as the basis for the wheel speed scheduled BTV compensator design, which is presented next. Then, experimental results obtained using a production ready prototype EMB and a brake dynamometer are presented to validate the proposed compensator design. The last section summarises the main results and provides some suggestions for future research.

## MODELLING OF AN ELECTROMECHANICAL BRAKE

A production-ready prototype EMB illustrated in Figure 1 is employed in this work to demonstrate the proposed BTV compensator. The EMB comprises a three-phase, permanent magnet synchronous motor, planetary gears, a ball screw, a floating calliper and control electronics. An experimentally validated simulation model for the EMB is presented in [9], and a procedure for obtaining the model parameters efficiently are presented in [10]. Additionally, high-bandwidth clamp force tracking can be achieved using the near-time-optimal clamp force control design proposed in [7].



Figure 1: The production-ready electromechanical brake prototype used in this work.

Taking into account of judder occurring during light braking, it can be assumed that the operating region of the judder compensator is confined to the vicinity of a small clamp force region. Hence, the compensator is designed based on a linearised EMB model with respect to the small clamp force region, taking the form of

$$\begin{bmatrix} \dot{\theta}_m \\ \omega_m \end{bmatrix} = \begin{bmatrix} 0 & 1 \\ -k_p & -k_d \end{bmatrix} \begin{bmatrix} \theta_m \\ \omega_m \end{bmatrix} + \begin{bmatrix} 0 \\ \frac{k_p}{k} \end{bmatrix} F_{cl,r} \quad (1)$$

$$F_{cl} = \bar{k} \theta_1,$$

where  $F_{cl}$ ,  $F_{cl,r}$ ,  $k_p$ ,  $k_d$ ,  $\bar{k}$ ,  $\theta_m$  and  $\omega_m$  are the brake clamp force, clamp force reference, proportional gain, derivative gain, linearised lumped stiffness coefficient, motor position and velocity respectively. Furthermore, consider the motor position  $\theta_m$  varies in the vicinity of  $\bar{\theta}_m$  during light braking, then the linearised lumped stiffness coefficient can be represented by

$$\bar{k} = k_1 \bar{\theta}_m^2 + k_2 \bar{\theta}_m. \quad (2)$$

To achieve a good clamp force tracking performance, proportional and derivative gains ( $k_p$  and  $k_d$ ) can be tuned according to the guidelines provided in [8].

$J$	Moment of inertia	$2.91 \times 10^{-4} \text{ kg.m}^2$
$k_1$	Stiffness coefficient	$-2.98 \times 10^{-1} \text{ N/rad}^3$
$k_2$	Stiffness coefficient	$3.29 \times 10 \text{ N/rad}^2$
$k_d$	Derivative gain	232.3
$k_p$	Proportional gain	5161.7
$r_d$	Brake disc radius	0.127 m
$T_{m\max}$	Motor torque limit	3 Nm
$\hat{\mu}$	Estimated coefficient of friction	0.484

Table 1: Parameters for the linearised EMB and BTV models

## MODELLING OF BRAKE TORQUE GENERATION

The brake torque,  $T_b$  is produced by applying a clamp force on both surfaces of a disc rotor via brake pads, and can be modelled as

$$T_b = 2\mu r_d F_{cl} + T_{btv}(\theta_d), \quad (3)$$

where  $\mu$ ,  $r_d$ ,  $T_{btv}$  and  $\theta_d$  are the coefficient of friction between brake pads and disc rotor, effective rotor radius, BTV and rotor rotational position respectively.

Furthermore, exact values of the coefficient of friction,  $\mu$  is not available during online implementation and it is affected by many environmental factors, such as temperature, speed and humidity. However, its variation is slow relative to the system dynamics (1), thus the discrepancy between the estimated friction coefficient,  $\hat{\mu}$  and the true friction coefficient,  $\mu$  can be assumed constant. This leads to the perturbed form of (3), given by

$$T_b = 2\hat{\mu}r_d F_{cl} + T_d + T_{btv}(\theta_d), \quad (4)$$

where  $T_d$  is the discrepancy in brake torque resulted from the estimated error in friction coefficient.

The BTV is caused by the geometry irregularities of the brake disc, therefore it must be periodic with respect to the disc rotation. By employing an  $n$ -order Fourier series expansion, the BTV is given by

$$T_{btv}(\theta_d) = \sum_{k=1}^n a_{b,k} \cos(k\theta_d + \phi_{b,k}), \quad (5)$$

where  $a_{b,k}$  and  $\phi_{b,k}$  represent the amplitude and phase-shift of the  $k$ -order harmonic respectively, while  $n$  is the maximum number of harmonic in the BTV model. The amplitude and phase-shift are unknowns, and are assumed to be time-invariant in the proceeding compensator design. However, these quantities may vary slowly relative to the disc rotations in practice.

The BTV model (5) is dependent on the disc rotor position  $\theta_d$ , which is not available in production vehicles. On the other hand, measured disc rotor speed  $\omega_d$  is readily available, as it corresponds to the wheel speed. Therefore, it is desirable to represent (5) in terms of  $\omega_d$  for the development of a BTV compensator that can be scheduled by wheel speed. For an appropriate choice of initial condition,  $w_k(0)$ , the  $k$ -harmonic of BTV can be represented by the following dynamics:

$$\begin{aligned} \dot{w}_k &= S_d(\omega_d)w_k \\ a_{b,k} \cos(k\theta_d + \phi_{b,k}) &= [1 \ 0]w_k, \end{aligned} \quad (6)$$

where

$$w_k = \begin{bmatrix} w_{k,1} \\ w_{k,2} \end{bmatrix}, \quad S_k(\omega_d) = \begin{bmatrix} 0 & k\omega_d \\ -k\omega_d & 0 \end{bmatrix}. \quad (7)$$

The sum of (6) for all harmonics from 1 to  $n$  renders an equivalent BTV model, which is governed by

$$\begin{aligned} \dot{\tilde{w}} &= \tilde{S}(\omega_d)\tilde{w} \\ T_{btv} &= \sum_{k=1}^n w_{k,1} = \underbrace{[1 \ 0 \ \cdots \ 1 \ 0]}_{n \text{ pairs}} \tilde{w}, \end{aligned} \quad (8)$$

where

$$\tilde{w} = [w_1^T \ \cdots \ w_n^T]^T, \quad \tilde{S}(\omega_d) = \text{diag}[S_1(\omega_d) \ \cdots \ S_n(\omega_d)] \quad (9)$$

Note  $\tilde{S}(\omega_d)$  is a square matrix comprises main diagonal blocks of  $S_k(\omega_d)$  and off-diagonal blocks of zeros.

Employing the EMB closed-loop system model (1), the brake torque expression (4) and the BTV model (8)-(9), the dynamics of the brake corner can be represented in the following form

$$\begin{bmatrix} \dot{x} \\ \dot{w} \end{bmatrix} = \begin{bmatrix} A & 0 \\ 0 & \tilde{S}(\omega_d) \end{bmatrix} \begin{bmatrix} x \\ w \end{bmatrix} + \begin{bmatrix} B_u \\ 0 \end{bmatrix} F_{cl,r}, \quad (10)$$

where the system state,  $x$  and the exogenous system state,  $w$  are defined by

$$x = [\theta_m \ \omega_m]^T, \quad w = [T_d \ w_1^T \ \cdots \ w_n^T]^T, \quad (11)$$

and the matrices are defined by

$$A = \begin{bmatrix} 0 & 1 \\ -k_p & -k_d \end{bmatrix}, \quad B_u = \begin{bmatrix} 0 \\ \frac{k_p}{k} \end{bmatrix}, \quad \tilde{S}(\omega_d) = \text{diag}[0 \ S_1(\omega_d) \ \cdots \ S_n(\omega_d)] \quad (12)$$

To aid the development of the BTV compensator, the brake torque tracking error dynamics is first analysed. To this end, define the torque tracking error as

$$e_b = T_b - T_{b,r} = Cx - D_{ew}w - T_{b,r}, \quad (13)$$

where  $T_{b,r}$  is the brake torque reference and the matrices are given by

$$C = [2\hat{\mu}_d \bar{k} \quad 0] \quad D_{ew} = \begin{bmatrix} 1 & 1 & 0 & \cdots & 1 & 0 \\ & & & \underbrace{\hspace{2cm}}_{n \text{ pairs}} & & \end{bmatrix}. \quad (14)$$

Furthermore, consider the change of variable,

$$\bar{x} = x - \begin{bmatrix} \frac{T_{b,r}}{2\hat{\mu}_d \bar{k}} \\ 0 \end{bmatrix}, \quad (15)$$

then the dynamics (10) can be rewritten as

$$\begin{bmatrix} \dot{\bar{x}} \\ \dot{w} \end{bmatrix} = \begin{bmatrix} A & 0 \\ 0 & S(\omega_d) \end{bmatrix} \begin{bmatrix} \bar{x} \\ w \end{bmatrix} + \begin{bmatrix} B_u \\ 0 \end{bmatrix} \bar{u} \quad (16)$$

$$e_b = \begin{bmatrix} C & D_{ew} \end{bmatrix} \begin{bmatrix} \bar{x} \\ w \end{bmatrix},$$

where  $\bar{u}$  is the compensating clamp force reference. Note the total clamp force reference consists of the compensating component,  $\bar{u}$  and a feedforward component scaled by the torque reference,  $T_{b,r}$ , that is

$$F_{cl,r} = \bar{u} + \frac{1}{2\hat{\mu}_d} T_{b,r}. \quad (17)$$

A compensator structure will be introduced in the next section to output the total clamp force reference.

## BRAKE TORQUE VARIATION COMPENSATOR DESIGN

An observer-based controller with parameter-varying terms is adopted for the compensator design, given by [11]

$$\begin{bmatrix} \dot{\hat{x}} \\ \dot{\hat{w}} \end{bmatrix} = \begin{bmatrix} A & 0 \\ 0 & S(\omega_d) \end{bmatrix} \begin{bmatrix} \hat{x} \\ \hat{w} \end{bmatrix} + \begin{bmatrix} B_u \\ 0 \end{bmatrix} F_{cl,r} + \begin{bmatrix} L_x \\ L_w \end{bmatrix} \left\{ \begin{bmatrix} C & D_{ew} \end{bmatrix} \begin{bmatrix} \hat{x} \\ \hat{w} \end{bmatrix} - e_b \right\} \quad (18)$$

$$F_{cl,r} = \begin{bmatrix} K_x & (\Gamma - K_x \Pi) \end{bmatrix} \begin{bmatrix} \hat{x} \\ \hat{w} \end{bmatrix} + \frac{1}{2\hat{\mu}_d} T_{b,r},$$

where  $\hat{x}$  and  $\hat{w}$  are the estimated values of  $\bar{x}$  and  $w$  respectively. Furthermore,  $K_x \in \mathfrak{R}^2$ ,  $L_x \in \mathfrak{R}^2$  and  $L_w \in \mathfrak{R}^{2n+1}$  are vectors chosen such that

$$A + B_u K_x \quad \text{and} \quad \begin{bmatrix} A + L_x C & L_x D_{ew} \\ L_w C & S + L_w D_{ew} \end{bmatrix} \quad (19)$$

are both Hurwitz. According to the output regulation theory, the terms  $\Gamma$  and  $\Pi$  have to satisfy the differential regulator equation [12], given by

$$\begin{aligned} \dot{\Pi} + \Pi S &= A\Pi + B_u \Gamma \\ \lim_{t \rightarrow \infty} (C\Pi + D_{ew}) &= 0. \end{aligned} \quad (20)$$

It can be shown that

$$\begin{aligned} \Pi(\omega_d) &= \begin{bmatrix} -1 & -1 & 0 & -1 & 0 & \cdots & -1 & 0 \\ 0 & 0 & -\omega_d & 0 & -2\omega_d & \cdots & 0 & -n\omega_d \end{bmatrix} \\ \Gamma(\omega_d, \dot{\omega}_d) &= \frac{1}{2\hat{\mu}_d k_p} \begin{bmatrix} -k_p & \omega_d^2 - k_p & -(\dot{\omega}_d + k_d \omega_d) & \cdots & (n\omega_d)^2 - k_p & -n(\dot{\omega}_d + k_d \omega_d) \end{bmatrix} \end{aligned} \quad (21)$$

satisfy the differential regulator equation (20). Due to space constraints, the steps for obtaining the expressions in (21) are not included here, but they can be found in [13]. Note that the compensator (18) and (21) are dependent on the wheel speed,  $\omega_d$  and acceleration  $\dot{\omega}_d$ . A block diagram for the BTV compensator, an EMB and a brake disc with torque variation is shown in Figure 2.

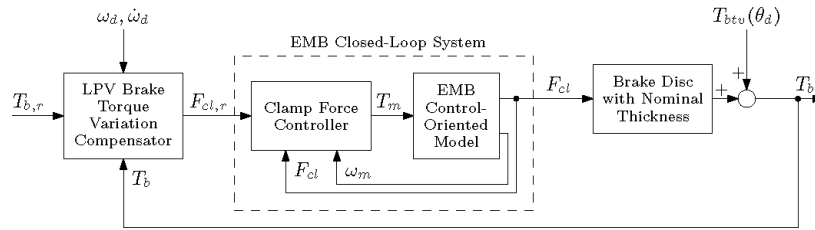


Figure 2: Block diagram of a compensator, an EMB and a brake disc with torque variation.

## RESULTS AND DISCUSSIONS

Experimental investigation of the proposed compensator is performed using a dedicated brake dynamometer and a production-ready prototype EMB illustrated in Figure 3. The experimental setup is also equipped with a PC laptop, a data acquisition system and a 42 V power supply. The forward-Euler method is used to discretised the proposed compensator with a sampling rate of 1000 Hz, and the discretised compensator is implementation on the PC. The PC is connected to the EMB via a CAN bus, where the clamp force command is sent to the EMB in real-time and the on-board measurements from the EMB are logged. Additionally, the PC is connected to the servo drive of the brake dynamometer, where the dynamometer speed can be varied online. Measurements from the brake torque sensor mounted on the dynamometer are also logged using the PC.



Figure 3: Brake dynamometer. The individual components are: 1. Dynamometer motor; 2. CAN cable; 3. Disc rotor; 4. EMB; 5. Thermometer connected to a thermocouple embedded in the brake pad; 6. Torque sensor.

The disc rotor employed for experiments was obtained from an in-service vehicle with brake judder. The maximum thickness variation of the disc is approximately 18  $\mu\text{m}$ , as shown in Figure 4. By analysing the Fourier components contained in the disc thickness variation profile, it is found that the first harmonic has the largest component, suggesting that a compensator design based on the first-order BTV model may be sufficient in implementation.

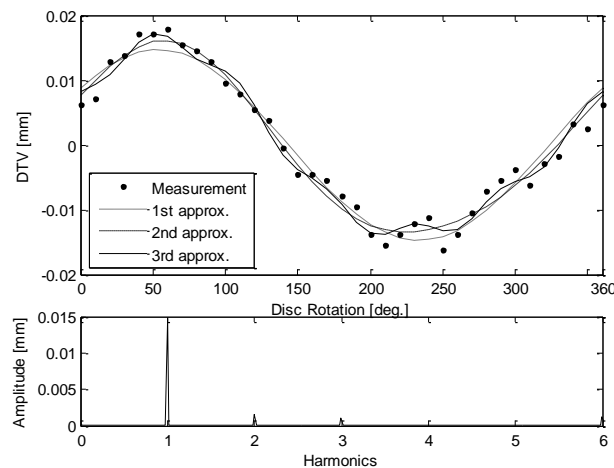


Figure 4: (Top) Disc thickness variation measurements and the first three orders of approximation. (Bottom) Amplitude spectrum of the disc thickness variation profile.

The first set of experimental test cases corresponds to braking under fixed wheel speed, which commonly occurs when light braking is applied to a vehicle descending a ramp. Figure 5 shows the brake torque and clamp force trajectories obtained for wheel speed of 60 rpm. The compensation started at 10 seconds, where the compensator was designed based on the first-order BTV model. It is evident that the BTV amplitude is attenuated when the compensator is activated, and a reduction in root mean square (RMS) of the BTV by 45% is demonstrated.

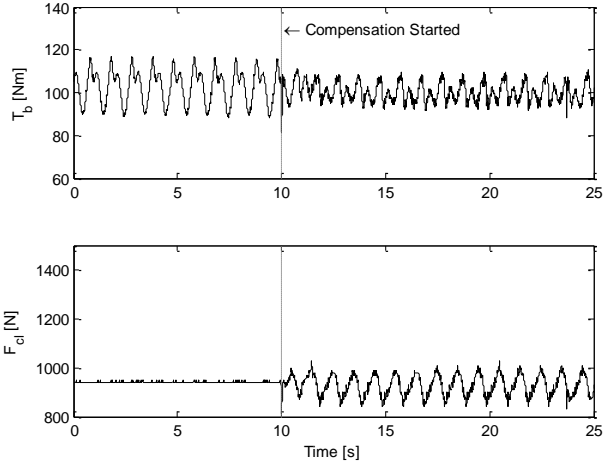


Figure 5: Brake torque variation compensation using the first-order compensator for a fixed wheel rotation speed of 60 rpm (1 Hz).

Figure 6 shows the amplitude spectrum of the uncompensated and compensated brake torque trajectories, where wheel speeds from 60 rpm (1 Hz) to 420 rpm (7 Hz) were tested. A first-order compensator scheduled with the wheel speed was employed in all cases. It is observed that the first-order harmonic (corresponds to the wheel speed) of the brake torque responses decreased with compensation, indicating that the first-order compensator was attenuating the first-order harmonic disturbance as intended.

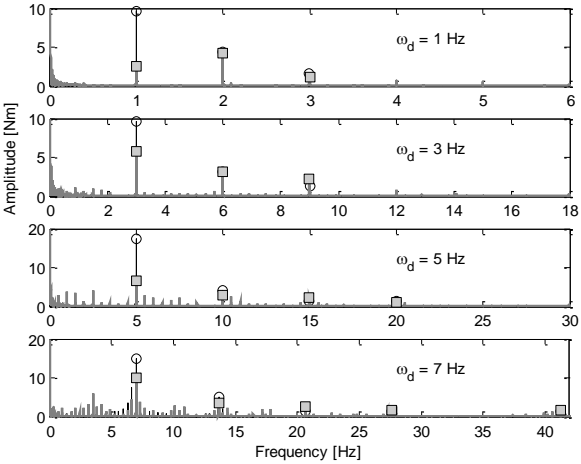


Figure 6: Amplitude spectrum of brake torque trajectories before (circles) and after (squares) compensation.

The second set of test cases corresponds to braking under varying wheel speed, which reflects the general braking scenarios. Figure 7 shows the brake torque compensation under fixed brake torque reference (at 100 Nm) and varying wheel speed, starting from 360 rpm (6 Hz) with a  $2 \text{ rad/s}^2$  deceleration. The compensator not only corrected the DC offset in the brake torque trajectory, it also reduced the RMS value of the BTV by 43%.

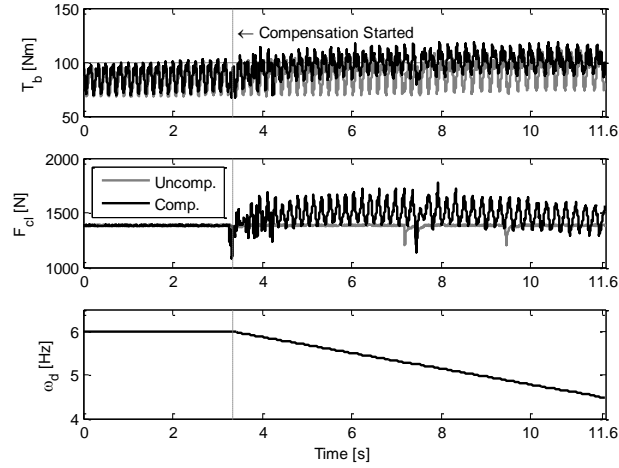


Figure 7: Brake torque responses with and without compensation under fixed brake torque reference (100 Nm) and varying wheel speed.

Figure 8 demonstrates brake torque compensation under varying brake torque reference and varying wheel speed. The brake torque reference was initially started at 100 Nm, and decreased to 20 Nm at 9.5 seconds, then gradually increased to 100 Nm from 12.5 seconds. The wheel speed began at 180 rpm (3 Hz), then gradually increased to 5 Hz from 9.5 seconds. It is observed that the amplitude of the BTV was attenuated, with a reduction of 33.5% in RMS value.

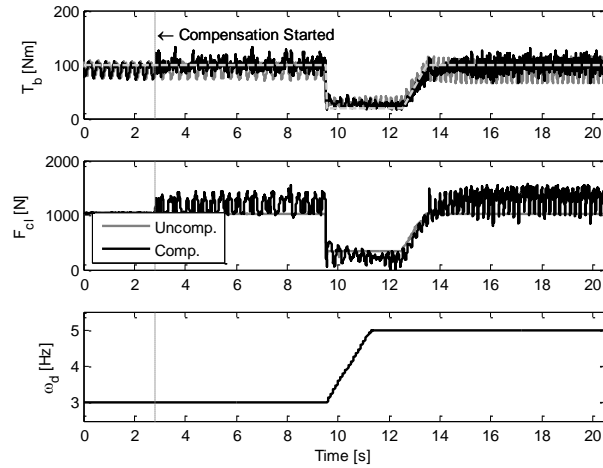


Figure 8: Brake torque responses with and without compensation under varying brake torque reference (dash grey line) and varying wheel speed.

## CONCLUSIONS

Taking advantage of the high-bandwidth closed-loop clamp force tracking offered by an electromechanical brake (EMB), an active solution for brake judder attenuation is proposed. The proposed judder compensation algorithm generates a compensating clamp force command online that attenuates the judder inducing brake torque variation. The proposed compensator design is very flexible and the order of the compensator can be easily modified to handle BTV with multiple harmonics. Preliminary experimental results demonstrate a reduction in root mean square (RMS) of the BTV by up to 45% using a first-order compensator, and the attenuation is consistent for both fixed and varying wheel speeds. Better performance is expected if higher order compensators are tested.

As opposed to the existing approach presented in [6] that requires wheel angular position measurements, the proposed algorithm is scheduled using wheel speed measurements readily available in production vehicles. Therefore, the proposed implementation alleviates the need of extra position sensors.

However, it is noted that the current design utilises brake torque measurements from the dynamometer, which may be lacking in production vehicles. Although brake torque measurement setups are often found in prototype vehicles, equipping this sensor in a near future production vehicle is not expected.

One possible direction for further research is the construction of a brake torque estimator, where the brake torque is estimated from mass, speed, longitudinal acceleration, and possibly road grade. Another idea that warrants further investigation is porting the proposed approach to hydraulic brakes, and to use pulse width modulation (PWM) techniques for high fidelity brake force regulation and tracking.

## REFERENCES

- [1] Abdelhamid, M. K. (1997), Brake judder analysis: Case studies, in 'SAE Conference Proceedings P', vol. 3, pp. 1225–1230. SAE Paper No. 972027.
- [2] Jacobsson, H. (2003), 'Aspect of disc brake judder', *Proceedings of the Institution of Mechanical Engineers, Part D: Journal of Automobile Engineering* **217**(6), pp. 419–430.
- [3] Kao, T. K., Richmond, J. W. and Douarre, A. (2000), 'Brake disc hot spotting and thermal judder: an experimental and finite element study', *International Journal of Vehicle Design* **23**(3/4), pp. 276–296.
- [4] Jacobsson, H. (2003), 'Disc brake judder considering instantaneous disc thickness and spatial friction variation', *Proceedings of the Institution of Mechanical Engineers, Part D: Journal of Automobile Engineering* **217**(5), pp. 325–342.
- [5] Engel, H. G., Hassiotis, V. and Tiemann, R. (1994), System approach to brake judder, in '25th FISITA Congress', pp. 332–339.
- [6] Lee, C. F. and Manzie, C. (2012), 'Adaptive Brake Torque Variation Compensation for an Electromechanical Brake', *SAE International Journal of Passenger Cars - Electronic and Electrical Systems* **5**(2), pp. 600–606. SAE Paper 2012-01-1840.
- [7] Lee, C. F. and Manzie, C. (2012), 'Near-time-optimal tracking controller design for an automotive electromechanical brake', *Proceedings of the Institution of Mechanical Engineers, Part I: Journal of Systems and Control Engineering* **226**(4), pp. 537–549.
- [8] Lee, C. F. and Manzie, C. (2012), 'High-Bandwidth Clamp Force Control for an Electromechanical Brake', *SAE International Journal of Passenger Cars - Electronic and Electrical Systems* **5**(2), pp. 590–599. SAE Paper 2012-01-1799.
- [9] Line, C., Manzie, C. and Good, M. (2008), 'Electromechanical brake modelling and control: from PI to MPC', *IEEE Transactions on Control Systems Technology* **16**(3), pp. 446–457.
- [10] Lee, C. F. and Manzie, C. (2013), Rapid Parameter Identification for an Electromechanical Brake, in 'Proceedings of the Australian Control Conference', pp. 391–396.
- [11] Saberi, A., Stoorvogel, A. and Sannuti, P. (2000), *Control of linear systems with regulation and input constraints*, Springer.
- [12] Ichikawa, A. and Katayama, H. (2006), 'Output regulation of time-varying systems', *Systems & Control Letters* **55**(12), pp. 999–1005.
- [13] Lee, C. F. (2013), Brake force control and judder compensation of an automotive electromechanical brake, PhD thesis, The University of Melbourne.